

A PROBABILISTIC APPROACH FOR ASSESSING DISCONTINUITIES IN STRUCTURAL STEEL COMPONENTS BASED ON CHARPY-V- NOTCH TESTS

Omar A. Ibrahim ^a, Dimitrios G. Lignos ^b and Colin A. Rogers ^c

^aAssistant Professor. Dept. of Structural Engineering, Alexandria University.
Lotfy El-Sied st. off Gamal Abd El-Naser - Alexandria, Alexandria Governorate 11432, Egypt
Tel: +20 3 5910052
email: omar.ibrahim@alexu.edu.eg

^bCorresponding author
Associate Professor. Dept. of Civil and Environmental Engineering, Ecole Polytechnique Fédérale de Lausanne (EPFL)
EPFL ENAC IIC RESSLab, GC B3 485, Station 18, CH-1015 Lausanne, Switzerland
email: dimitrios.lignos@epfl.ch
Tel. +41 21 693 2427
Fax. +41 21 693 2868

^cAssociate Professor. Dept. of Civil Engineering and Applied Mechanics McGill University
Macdonald Engineering Building 817 Sherbrooke Street West Montreal, QC, Canada, H3A 0C3
email: colin.rogers@mcgill.ca

Abstract

Available acceptance and rejection criteria for discontinuities in steel components of a welded assembly focus only on a minimum limit for the steel fracture toughness and a maximum limit for the size of the discontinuity. However, other critical parameters such as the uncertainty in the fracture toughness value and the working stress type in the steel component are not taken into account. The uncertainty in the fracture toughness increases as the steel component becomes thicker, which in combination with an increase in the demand for thick steel components in construction is cause for concern. Proposed in this paper is a probabilistic approach for the assessment of discontinuities that accounts for the variability of the fracture toughness throughout the material as well as the working stress type. A database of Charpy-V-notch (CVN) impact test results was developed for steel plates of different grades, thicknesses and at different temperatures. Each dataset was fitted with a statistical distribution, which was then converted to the corresponding fracture toughness. Through logistic regression and linear fracture mechanics an expression was developed to calculate the probability of a discontinuity's stress intensity factor exceeding the fracture toughness of the material. By determining an acceptance limit of this probability value based on the working stress type of the component and assembly (importance) the proposed approach can be implemented to accept or refuse a discontinuity in a steel component.

Keywords: Discontinuities acceptance criterion, Charpy-V-notch, Fracture toughness uncertainty, Crack initiation in steel, Logistic regression.

1 Introduction

Welding is one of the most popular steel joining methods in North America. The combination of the tensile residual stresses associated with the welding procedures for steel assemblies and the discontinuities already present in the steel component prior to welding can lead to crack initiation. The crack initiation primarily depends on three parameters: the discontinuity size and type; the applied stress (welding residual stress level); and the fracture toughness of the steel material at the corresponding temperature [1]. The fracture toughness of a material is often used to define its ability to withstand crack initiation; one of the most common methods of calculating fracture toughness is through the Charpy-V-Notch (CVN) absorbed energy value. Current assessment criteria for discontinuities in steel plates [2-5] have been written such that only maximum allowable discontinuity sizes and minimum CVN values according to the steel grade are considered; the significance of other parameters such as the position and type of the discontinuity as well as the applied stress level are not addressed. Moreover, the fracture toughness of steel is not constant within a steel plate [6, 7]. This is another issue that is not addressed in today's specifications [2-5].

In recent years, there is an increasing need for the use of thick steel plates in high-rise steel frame buildings as well as steel bridges. As the thickness of a steel plate increases its fracture toughness decreases, and the variation in the fracture toughness within the same component increases [7, 8]. It is understood that the uncertainty of the fracture toughness value through the thickness of a steel plate should be quantified, and as such should be considered by current welding and steel construction specifications. Furthermore, in the process of evaluating discontinuities, current specifications [2-5] should take into account the importance of a steel component as part of a steel

structure (i.e., fracture critical). The working load that a steel component experiences is also another important consideration (i.e., compressive only or compressive/tensile). For instance, in a building, exterior columns experience compressive as well as tensile stresses due to dynamic overturning effects during an earthquake. Interior columns are more likely to be subject to compressive stresses alone, or certainly much lower levels of tensile stresses than exterior columns. Accordingly, discontinuities at the butt-welded splices of exterior columns are more critical than at the same connections for interior columns; which requires distinction in the discontinuities acceptance criteria from non-critical components. Correspondingly, a reliable assessment of discontinuities in steel plates should incorporate the uncertainty in the steel fracture toughness value, the working stress level, the size, position and type of the discontinuity as well as the importance level of the steel component and assembly. This can be achieved through using an approach conceptually similar to that of performance-based building design.

In current North American code provisions [2-5] the acceptance of a steel component to be used in construction depends on the steel grade and its CVN value. The latter is relied on to estimate the fracture toughness of the corresponding steel material. For instance, according to ANSI/AISC 360-10 [2], CAN/CSA-S16-14 [3], AWS D1.1 [4] and CAN/CSA-W59 [5] the CVN value for ASTM A572 Gr.50 [9] steel (i.e., nominal yield stress $f_y = 345\text{MPa}$) and ASTM A913 Gr.65 [10] steel (i.e., $f_y = 450\text{MPa}$) should not be less than 27 and 54 Joules at 21°C, respectively. These criteria are often used assuming the fracture toughness at a given temperature is consistent for all locations in the component, which may not be a valid approach (see Section 3). Furthermore, for cracks induced by the welding procedure, “Table 6.2” and Figures “(6.1-6.3)” of AWS D1.1.2010 [4] illustrate the acceptable crack sizes in a weld based on ultrasonic and radiographic tests,

respectively. Based on linear fracture mechanics, a crack is likely to initiate if the stress intensity factor at the crack tip is greater than the fracture toughness of the steel material. The stress intensity factor depends on the crack shape and size as well as the applied stress [11, 12]. The fracture toughness of the material is calculated from the CVN absorbed energy value of the material [8]. The accepted discontinuity size is 18mm for a 25mm weld size [see “Figure 6.1” in [4]]; considering a working tensile stress of 200MPa [60% of the yield stress of ASTM A572 Gr.50 [9] Gr.50 steel] and a through thickness discontinuity, the corresponding stress intensity factor is $57\text{MPa}\cdot\sqrt{\text{m}}$ [11, 12]. However, acknowledging the CVN limit for ASTM A572 Gr. 50 (i.e., $f_y = 345\text{ MPa}$) steel, mentioned previously, the corresponding minimum fracture toughness limit is $56\text{MPa}\cdot\sqrt{\text{m}}$ [8]. This means that although the discontinuity size is deemed acceptable according to the welding provisions in AWS D1.1 [4] and the CVN limit is met [2, 3], by employing basic concepts of linear fracture mechanics it can be demonstrated that a crack will most likely initiate along the weld. This simple example indicates that a more comprehensive approach is required to assess cracks and discontinuities present in a welded assembly. This approach should take into account the uncertainty in the fracture toughness value along with the influence of the parameters affecting the stress intensity factor. In addition, discontinuity tolerance limits should be set as a function of the probability of the discontinuity stress intensity factor to exceed the fracture toughness of the material. The same limits should be based on the importance as well as the working load of the structural steel component.

Proposed in this paper is a practical approach for the assessment of discontinuities in steel plates to determine their critical sizes; taking into account the uncertainty in the value of the material fracture toughness. This was achieved in part through implementing statistical procedures to

develop CVN fragility curves based on a database of CVN test results that includes: (a) various steel grades; (b) a range of temperatures; and (c) plates of different thickness. The CVN database was divided into subsets according to the material and testing conditions. A statistical treatment of the data subsets was also employed, accounting for various sources of epistemic uncertainty, to determine a statistical distribution that fits the assembled datasets. Fragility curves for crack initiation were then developed for each subset. Finally, using logistic regression [13] a predictive formula was developed to compute the probability of crack initiation given the stress intensity factor, temperature, material type and plate thickness. The impact of parameters such as the crack type, steel material grade, temperature, crack position and plate thickness, on the probability of the crack to initiate was investigated thoroughly. To the best of our knowledge there are no prior studies that utilize the uncertainty associated with the fracture toughness of a steel material, as a result of the aforementioned parameters, in order to develop a probabilistic approach for assessing cracks and discontinuities existing in a steel component.

2 Outline of the Proposed Methodology and Fragility Curves Development

The proposed methodology is based on a CVN database that was first developed as part of this paper. This database, discussed in detail in Section 3, contains information regarding measured CVN values from different types of steel materials. Based on this database, in Section 4 fragility curves are developed for each steel type based on the maximum likelihood approach [13, 14]. These curves are used to compute the probability of reaching or exceeding the CVN value given the thickness and temperature of the corresponding steel component. The epistemic uncertainty of the aforementioned fragility curves, induced by the test conditions, is also addressed. The corresponding fracture toughness of each subset is obtained from the CVN value. Through the use

of logistic regression, predictive equations were proposed, with which one can compute the probability of crack initiation under a specified stress, crack size and type; this aspect of the methodology is discussed in Section 5.

3 CVN Database Development

The CVN database comprised tests conducted by Suwan [7] for ASTM A572 Gr.50 [9] steel ($f_y = 345$ MPa) and ASTM A588 Gr.B [15] ($f_y = 345$ MPa); as these tests included different materials, thicknesses and test temperatures. Additional tests were conducted at McGill University for ASTM A572 Gr. 50 steel ($f_y = 345$ MPa) and ASTM A913 Gr. 65 steel ($f_y = 450$ MPa) [6, 16], to include additional test temperatures to those done by Suwan for A572 Gr.50 steel, and to add another steel grade that is also used in construction. The CVN tests conducted by Suwan according to ASTM A370 [17] resulted in 672 absorbed energy values for ASTM A572 Gr. 50 steel and 777 for ASTM A588 Gr. B steel. The specimens, obtained from four different steel mills in the United States of America, were divided into four groups according to the corresponding steel plate thickness (<20mm, 20 to 40mm, 40 to 65mm and 65 to 100mm). The testing temperatures were -18, 4 and 21 °C. Each specimen was machined from a position parallel to the rolling direction of the parent plate.

The CVN dataset provided by Suwan [7] was expanded through the inclusion of CVN tests conducted by Ibrahim et al. [6] according to ASTM A370 [17]. The new dataset included 88 specimens made from ASTM A572 Gr. 50 steel plate from one mill in the USA at a temperature range of -60, -40, 0, 60 and 81 °C. All the specimens were taken from a position perpendicular to the rolling direction of the parent plate. Since the specimens were extracted from a 75mm thick steel plate, these results were included in the thickness group ranging from 65 to 100mm. In

addition, 114 specimens obtained from ASTM A913 Gr. 65 steel W360×237 wide flange sections by Nikolaidou et al. [16] were incorporated as part of the study. A total of 56 of these specimens were taken from a position in the flanges parallel to the rolling direction of the W section, while the rest were obtained from a position in the flanges perpendicular to the rolling direction. Due to a nominal flange thickness of 30 mm this data subset was considered in the thickness group 20-40mm. These CVN specimens were tested at 0, 21, 48 and 69 °C. Tables 1 and 2 summarize the basic statistical quantities of the dissipated energy associated with the mean, μ , 5th and 95th mean percentiles (i.e., $\mu_{5\%}$, $\mu_{95\%}$) and the associated logarithmic standard deviations, β , of the CVN tests included in the database. The scatter in the reported CVN values for each dataset necessitates the use of a probabilistic approach for estimating the probability of reaching or exceeding each CVN value. From this database, it was possible to investigate the effects of temperature, the material type and the plate thickness on the fracture toughness of a steel component.

4 Statistical treatment of the CVN data

In order to compute the probability of crack initiation through a steel plate from the obtained CVN data, each subset was represented by a statistical distribution which was fitted following the rigorous goodness-of-fit approaches discussed in Section 4.1. Furthermore, the effect of epistemic uncertainty on the CVN results was considered with the approach discussed in Section 4.2.

4.1 Distribution fitting

The CVN values from each group discussed in Section 3 were evaluated using a Kolmogorov-Smirnov's (K-S) goodness-of-fit test [14] to develop the optimal probabilistic distribution that fits the data; as the K-S test is independent of the function being tested and the sample size. Other

statistical hypothesis tests can also be used, such as the chi-square goodness-of-fit test [18]. However, the chi-square test requires a sufficient sample size in order for the results to be valid. The lognormal, the Weibull and the exponential probability distribution functions were employed to express the likelihood of reaching or exceeding a CVN value given a temperature and plate thickness. The parameters of these distributions were computed based on the method of maximum likelihood [14]. The maximum difference between the empirical distribution and each statistical distribution and the 5% significance level of the K-S test is shown in Table 3 for two different thicknesses (less than 20mm and 20-40mm) of the ASTM A572 Gr. 50 CVN tests conducted by Suwan [7]. The Weibull distribution has the least difference with the empirical results and the cumulative probability distribution of the CVN data. However, the lognormal distribution slightly exceeds the KS-test limit only for thicknesses less than 20mm at 4°C. A lognormal distribution was ultimately employed because CVN values are always positive and most of the individual CVN data has a skewed distribution with a longer tail for upper values. A summary of the lognormal means (μ) and logarithmic standard deviations (β) of the energy values for all the subsets discussed in Section 3 are shown in Tables 1 and 2. The mean of a distribution increases with the increase of temperature as would be expected. Also, the standard deviations reflect how sensitive the CVN value is with respect to the location in the steel plate and the thickness of the steel plate from which the CVN coupon was taken.

Figures 1a and 1b show the fitted lognormal probability distributions (solid black line) of the empirical distribution CVN subsets of the A572 Gr. 50 steel at 0 and -40°C, respectively. As anticipated, with the decrease in temperature the steel material becomes brittle and the probability of reaching or exceeding a specified CVN value decreases. For example, the probability of

reaching or exceeding the CVN limit based on the current code provisions in North America [2-5] at 0°C is 99% and at -40°C is 80%. Similarly, Figures 1c and 1d illustrate the lognormal probability distributions of the empirical distribution CVN subsets for ASTM A913 Gr. 65 steel at 0°C in the positions parallel and perpendicular to the rolling direction, respectively. The probability of reaching or exceeding a specified CVN value for specimens oriented parallel to the rolling direction is larger than that for specimens located perpendicular to the rolling direction of the steel. As such, the probability of reaching or exceeding the CVN limit based on the current code provisions in North America [2-5] for specimens parallel to the rolling direction is 68% and for specimens perpendicular to the rolling direction is 10%.

4.2 Incorporation of epistemic uncertainties in the fragility curves

The fragility curves presented in Section 4.1 only account for the specimen-to-specimen variability; it is possible to subsequently incorporate the effect of epistemic uncertainty into these developed fragility curves. One source of epistemic uncertainty arises from the finite sample of specimens included per group. Another source is the material variability; such that material properties are not the same for all the plates that were obtained from the same mill, in addition to the fact that the plates and wide flange sections, along with the corresponding CVN specimens, were from different mills. Another source of epistemic uncertainty is the difficulty to fully control the temperature conditions during each CVN test. In order to include the effect of these uncertainties on the CVN results, a 5% and 95% confidence interval was considered. The values of the shifted mean and standard deviations for the lognormally distributed data discussed earlier were estimated based on Equations 1 and 2, respectively [19, 20]:

$$\text{Shifted Means} = \left(\overline{CVN} - \frac{\bar{\Delta}_{CVN}}{2} \right) \cdot \exp \left(\pm t_{\alpha/2} \cdot \frac{\sigma_{CVN}}{\sqrt{n}} \right) \quad (1)$$

$$\text{Shifted standard deviations} = \left(\frac{(n-1) \cdot \sigma_{CVN}^2}{X_{\alpha/2, n-1}^2} \right)^{1/2} \quad \text{and} \quad \left(\frac{(n-1) \cdot \sigma_{CVN}^2}{X_{1-\alpha/2, n-1}^2} \right)^{1/2} \quad (2)$$

Where, \overline{CVN} is the mean of the CVN subset under consideration, $\bar{\Delta}_{CVN}$ is the mean of the increment between the CVN values, σ_{CVN} is the standard deviation of the lognormal distribution, n is the number of specimens, $t_{\alpha/2}$ is the value of the student- t -distribution such that the probability of occurrence is $\alpha/2$ at number of specimens n ; $X_{\alpha/2, n-1}^2$ is the value of the Chi-Squared-distribution such that the probability of occurrence is $\alpha/2$ at $n-1$ degrees of freedom; $X_{1-\alpha/2, n-1}^2$ is the value of the Chi-Squared-distribution such that the probability is $1-\alpha/2$ at $n-1$ degrees of freedom and α is the required confidence interval. Figure 1 shows an example of the shifted fragility boundaries for ASTM A572 Gr. 50 steel (Figures 1a and 1b) and ASTM A913 Gr. 65 steel (Figures 1c and 1d) with a 5% and 95% confidence interval. In the case of ASTM A913 steel for example, from Figure 1d the probability of exceedance is 10% for an AISC [3] specified CVN value of 54 Joules, whereas if the epistemic uncertainty were accounted for the probability of exceedance would be in the range from 0 to 70%. This range indicates the sensitivity of CVN test data to testing conditions and that the probability of exceeding a specified CVN value may be better or worse as illustrated by the shifted distributions. Similar findings hold true for the rest of the subsets discussed in Section 3. Tables 1 and 2 show the corresponding shifted means ($\mu_{5\%}$ and $\mu_{95\%}$) and logarithmic standard deviations ($\beta_{5\%}$ and $\beta_{95\%}$) to compute the shifted boundaries for each group. Given the statistical distribution of each CVN subset the corresponding fracture toughness distribution can be developed. Subsequently, based on linear fracture mechanics one

can compute the stress intensity factors for different crack sizes and at different tensile stress levels; thus the crack initiation fragility curves can be developed as discussed in Section 5.

5 Computation of Probability of Crack Initiation

A probabilistic approach to assess cracks and discontinuities based on the material fracture toughness uncertainty requires the development of crack initiation fragility curves. These curves are used to compute the probability of the material fracture toughness being less than the stress intensity factor of a crack, for a given crack size and a stress level. The same curves form the basis to establish expressions that may be used to compute the probability of crack initiation under a specified stress level and crack size (i.e., stress intensity factor). The first step for developing the crack initiation fragility curves is estimating the fracture toughness distribution for each subset from the obtained lognormal distributions for all the CVN subsets summarized in Tables 1 and 2. Knowing that the CVN test is essentially an impact test, the computed output from the CVN test corresponds to the dynamic fracture toughness [8]. For lower shelf temperatures, the static fracture toughness is of the same value but at a lower temperature such that the temperature shift is computed from Equation 3 [8]:

$$\begin{aligned} T_s &= 102 - 0.12 f_y, & \text{for } 250 \text{MPa} < f_y \leq 965 \text{MPa} \\ T_s &= 0, & \text{for } f_y > 965 \text{MPa} \end{aligned} \quad (3)$$

Where T_s is the temperature shift ($^{\circ}\text{C}$) and f_y is the yield stress of the material in MPa. For upper shelf temperatures there is no temperature shift required to transfer from the dynamic to the static fracture toughness [8]; due to the increase in the material ductility at these temperatures. The fracture toughness is given by the following empirical equations,

$$K_{I_d} = \sqrt{0.64 \times CVN \times E}, \quad \text{For lower shelf temperatures} \quad (4)$$

$$\left(\frac{K_{I_c}}{f_y}\right)^2 = 0.646 \left(\frac{CVN}{f_y} - 0.0098\right), \quad \text{For upper shelf temperatures} \quad (5)$$

Where K_{I_d} is the dynamic fracture toughness (KPa. \sqrt{m}), K_{I_c} is the static fracture toughness (MPa. \sqrt{m}), CVN is the absorbed energy measured from Charpy-V-Notch tests (Joules) and E is the modulus of elasticity of the steel material (KPa). Alternative methods to compute the material's fracture toughness can also be found according to the structural integrity assessment procedures for European industries (SINTAP) [21] as well as the British specification for the assessment and acceptability of flaws in metallic structures (BS 7910) [22].

The statistical distribution of the static fracture toughness at 0 and 21°C was interpolated based on the ASTM A572 Gr. 50 steel subsets for the tests conducted at McGill University [6, 16]. The values of the static fracture toughness at -60 and 60°C are at the start and end of the transition zone, respectively. According to the results of the tests conducted by Ibrahim et al. [6] it can be assumed that the relation between the static fracture toughness and the temperature is linear in the range from -60 and 60°C; therefore, the relationship between the fracture toughness and the probability of reaching or exceeding a given fracture toughness at any temperature between -60 and 60°C can be linearly interpolated between the lognormal distributions at -60 and 60°C. From the developed lognormal distributions, the effect of the material type, plate thickness, temperature, and grain direction on the fracture toughness is considered. Moreover, for the estimation of the stress intensity factor, the fracture mode is considered to be “Mode I” [1]. The stress intensity factor depends on the crack type and is computed according to the applied tensile stress (σ) and the crack size (a). Five crack types are considered in this paper, as shown in Figure 2: 1) through

thickness crack in a finite plate (by comparing the crack size (a) to the plate thickness (t)); 2) through thickness crack in an infinite plate (by comparing the crack size (a) to the plate width); 3) edge crack in a finite plate (by comparing the crack size (a) to the plate thickness (t)); 4) edge crack in an infinite plate (by comparing the crack size (a) to the plate width); and 5) embedded circular crack. The stress intensity factor for each crack type can be calculated, in the same order for each crack type, according to Murakami [11] and Tada et al. [12] from the Equations 6 to 10:

$$K = \sigma\sqrt{\pi a} \cdot \sqrt{\sec\left(\frac{\pi a}{2b}\right)}, \quad \text{Through thickness crack in a finite plate} \quad (6)$$

$$K = \sigma\sqrt{\pi a}, \quad \text{Through thickness crack in an infinite plate} \quad (7)$$

$$K = 1.12\sigma\sqrt{\pi a} \cdot f\left(\frac{a}{b}\right) \quad \text{Edge crack in a finite plate} \quad (8)$$

$$f\left(\frac{a}{b}\right) = 0.236(1-a/b)^4 + \frac{0.765+0.236a/b}{(1-a/b)^{3/2}}$$

$$K = 1.12\sigma\sqrt{\pi a}, \quad \text{Edge crack in an infinite plate} \quad (9)$$

$$K = 1.13\sigma\sqrt{a}, \quad \text{Embedded circular crack} \quad (10)$$

in which, σ is the applied stress level for fracture mode I (MPa); a is equal to the crack length for edge cracks, half of the crack length for through thickness cracks and the radius of the embedded circle for an embedded circular crack (mm); b is the thickness of the finite plate in the direction of the crack for edge crack and half the plate thickness for through thickness cracks (mm); and $f(a/b)$ is a factor depending on the ratio between a and b . The stress intensity factor is calculated at different tensile stress levels and crack lengths for each crack type based on Equations 6 to 10. The probability of having a material fracture toughness less than or equal to the stress intensity factor

of a crack, for a given crack size and a tensile stress level (crack initiation fragility curves) can be calculated from the statistical distribution of the static and dynamic fracture toughness.

Based on the developed crack initiation fragility curves of the subsets discussed in Section 3, mathematical expressions were developed based on logistic regression [11] to calculate the probability of crack initiation for each subset. These expressions give the relation between the probability of crack initiation through a material, at a given temperature, plate thickness and position, and the stress intensity factor of a given crack size and a tensile stress level. The logistic regression was conducted in MATLAB R2012b [23] in order to calculate the constants of Equation 11:

$$P(K_I < K | K = K_i) = \frac{e^{B_0 + B_1 K_i}}{1 + e^{B_0 + B_1 K_i}} \quad (11)$$

in which, K is the calculated stress intensity factor given the crack size and the applied stress level, K_I is the fracture toughness of the material and B_0 and B_1 are constants. Tables 4 – 6 summarize the values of B_0 and B_1 for each subset, and list the deviance and maximum residual for all the subsets. From Table 6, for the subset of ASTM A913 Gr. 65 steel, the deviance ranges from 0.14 at 69°C in the direction parallel to rolling to 8.21 at 0°C in the perpendicular direction. As the deviance alone is not representative of the goodness-of-fit, the maximum residual for each set was also considered. The maximum residual ranges from 2.1% for the interpolated subset of ASTM A572 Gr. 50 steel at 21 °C to 9% for the subset of ASTM A572 Gr. 50 steel at -18°C for thickness group (40-65mm). Figure 3 shows a comparison between the crack initiation fragility curves and Equation 11. According to Tables 4 – 6 the average deviances are 1.98, 1.14, 2.54 and 3.37,

respectively, and the average maximum residuals are 0.05, 0.04, 0.06 and 0.07, respectively for all four material datasets.

Subsequently, the impact of the crack type, material type, the plate temperature, grain direction (a function of the rolling direction) and the plate thickness on the probability of crack initiation was evaluated through surface probability plots; in which the crack size and the applied stress level are on the horizontal axes and the probability of crack initiation on the vertical axis (Figure 3). The reason for using surface plots is to include the applied stress level in the graph and to examine its influence on the probability of a crack with a given size to initiate, as this parameter is also ignored by current specifications [2-5]. The stress intensity factor for the cracks in a finite plate depends on the ratio between the crack length and the material thickness a/b as shown in Equations 6 and 8; therefore, for each subset two surface plots were developed as an upper and lower bound of the probability of crack initiation. As an example, for the thickness group (20-40mm) a/b for the lower and upper bounds surface plots is $a/20$ and $a/40$ respectively. Figure 4 shows the upper and lower bounds of the probability of initiation of cracks in a finite plate for ASTM A572 Gr. 50 steel for thickness group (65-100mm). Two temperatures are given for each plot to (T1/T2) in Figures 4 to 8; where T1 is the temperature for the dynamic loads and T2 is the temperature for the static loads. Sections 5.1 to 5.4 contain a discussion of the impact of each parameter on the probability of crack initiation of a crack type.

5.1 Impact of crack type

The probability of crack initiation is sensitive to the crack type (Figure 2). Figure 4 shows the difference in the probability of crack initiation between an edge crack (Figure 2b crack type 3) and a through thickness crack (Figure 2b crack type 1) for ASTM A572 Gr. 50 steel plates. An edge

crack is more likely to initiate than a through thickness crack for the same stress level because a through thickness crack is confined by the steel material from both sides, while for an edge crack this is not the case. That is, an edge crack requires less energy to break the material bonds than that needed in a through thickness crack. After evaluating the other types of cracks in the same manner, the embedded circular crack type is the least sensitive to initiate under the same conditions compared to edge and through thickness cracks. It is implied that assessing a crack based on its size alone is not sufficient. This has direct implications into the current code provisions [2-5] that specify the allowable crack size in welds without considering the crack type.

5.2 Impact of material type

The influence of the material type on the probability of crack initiation is described herein. Figure 5 shows surface probability plots for ASTM A572 Gr. 50 and ASTM A913 Gr. 65 steels for the same plate thickness, crack type and similar temperature. The probability of crack type 4 initiation for the A913 Gr. 65 material was higher than that of the A572 Gr. 50 material. This was attributed to the higher nominal yield stress of the A913 Gr. 65 steel. The current code provisions [2-5] consider the material impact on the probability of crack initiation by specifying a higher CVN minimum requirement for ASTM A913 steel (Section 1). Furthermore, by converting the acceptance limits to the proposed probabilistic approach the maximum acceptable stress intensity factors calculated from the CVN minimum requirements would be 85 and 60 MPa. \sqrt{m} for ASTM A913 and A572 steels, respectively. By substituting these values in Equation 11, the probability of crack initiation is 29% and 0.7% for ASTM A913 and A572 steels, respectively. This means that current specification limits for ASTM A572 grade 50 steel (27J) correspond to a high probability of crack initiation according to the statistical distribution of the CVN values of this

steel grade. While specification limits for ASTM A913 Gr. 65 steel (54J) correspond to a low probability of crack initiation according to the statistical distribution of the CVN values of this steel grade. Accordingly, there is no consistency between the CVN value acceptance limits for different steel grades in current specifications [2-5]. Figure 5 shows a comparison between the probabilities of crack initiation surface plots for both steel grades for an edge horizontal crack at a temperature range from 0°C to 4°C. This illustrates that under the same conditions A913 grade 65 quenched steel has higher probability of crack initiation than A572 grade 50 steel.

5.3 Impact of temperature and grain direction

The effect of temperature and grain direction on the probability of crack initiation is presented given a stress level. Typically, with the decrease in temperature, the material becomes more brittle and the fracture toughness decreases [1]. This decrease in the fracture toughness leads to an increase in the probability of crack initiation. Figure 6 shows the increase in the probability of the crack initiation with the decrease in temperature for ASTM A572 Gr. 50 steel. The CVN specimens for the ASTM A913 Gr. 65 material were milled from both the direction parallel and perpendicular to the rolling direction. It is assumed that the grain structure in the rolling direction is elongated, while in the perpendicular to rolling direction the grain structure is shortened. Figure 7 shows the probability of crack initiation at upper and lower shelf temperatures for ASTM A913 Gr. 65 steel in the directions parallel and perpendicular to the rolling direction (long and short grains directions respectively). The difference between the probability of crack initiation in the lower and upper shelf temperatures in the long grain direction is always higher than that in the short grain direction. This is attributed to the fact that the inter-grain connections in the long direction are stronger than those in the short direction [24]. It is worth mentioning that current code provisions [2-5] have no

distinction for crack limitations in different directions; however, AWS D1.1 [4] acknowledges that the rolling process causes the base metal to have different mechanical properties in the orthogonal directions. It is not clear if the provisions of the current specifications [2-5] were established considering a lower bound or an upper bound of the CVN values; hence, the code provisions [2-5] should include a distinction between the crack limitations in the long and short grain directions to avoid over or under estimating the CVN acceptance limits. One way to include these parameters in the assessment of discontinuities is through the approach proposed herein.

5.4 Impact of plate thickness

According to current North American steel and welding code provisions [2-5] a material discontinuity is evaluated in the same way regardless of the steel plate thickness. However, it is generally known that when the steel plate thickness increases, the grain structure present through the steel plate thickness is not as effectively rolled as are the grains on the outer surface of the material [24]. This can lead to an increase in the probability of crack initiation [11, 12]. The proposed methodology for the evaluation of crack initiation given the stress level is able to consider this material variation; an important issue given the increasing use of thick steel plates in construction. Figure 8 shows the probability of crack initiation for the four different thickness groups that are summarized in Table 1 for ASTM A588 Gr. B steel. While the steel plate thickness increases, the probability of crack type 4 initiation increases. This indicates that the current provisions for acceptance criteria of discontinuities should be re-evaluated and a distinction based on steel plate thickness should be incorporated.

The proposed methodology for evaluating the likelihood of crack initiation includes consideration of the effect of the material type, the plate temperature, the grain direction and the plate thickness.

In particular, Equation 11 and Tables 4 – 6 reflect these effects. Code provisions or a designer can define a probability limit in order to determine whether to accept a particular steel component given the size of its discontinuities. In the definition of this limit it is necessary to consider the importance of the structure or the steel assembly to be welded, as well as the stress level to which it will be subjected. As an example, the recommended probability of crack initiation limit should not be more than 5% based on the probability of exceeding the prescribed CVN limit [2-5] for ASTM A572 Gr. 50 steel.

6 Summary and Conclusions

A new methodology is proposed to calculate the probability of a crack to initiate through a steel component accounting for the uncertainty in its fracture toughness. The development of this approach is based on a database of CVN values from steel plates and wide-flange sections of different thickness and grade, with specimens obtained from different locations with various grain directions and tested over a range of temperatures. The datasets have undergone rigorous statistical framework comprising the goodness-of-fit of the describing statistical distribution and the epistemic uncertainty from the testing procedure. Through logistic regression, expressions were developed to calculate the probability of a crack to initiate through a steel component. Consequently, the impact of the different parameters was investigated. From this assessment, the following conclusions hold true:

- An edge crack is more prone to initiate under a specified stress level than a through thickness crack, which in turn has a higher probability of initiation compared with an embedded circular crack. Therefore, present code provisions [2-5] should assess a crack based on its type as well as its size.

- A high strength steel material has a higher probability of crack initiation than a low strength steel material. Present code provisions [2-5] consider this issue. However, the uncertainty associated with the fracture toughness value, which increases with the respective steel strength, is currently neglected. This could lead to the acceptance of a material CVN value based on a test result, which may not be valid for specimens from a different location in the same material. Hence, this can be avoided by including the uncertainty of the CVN value of a material in the acceptance criteria.
- With an increase in temperature the probability of crack initiation decreases until the maximum fracture toughness of the steel material is reached. The difference between the probability of crack initiation in the lower and upper shelf temperatures in the direction parallel to rolling is always higher than that in the perpendicular direction.
- The greater the steel plate thickness the larger the scatter in the fracture toughness values of a steel component. This is attributed to the effectiveness of the rolling procedure from the plate surface to the centerline of its thickness.

The proposed approach can be employed to assess discontinuities and cracks in a steel component, which are often the result of welding and/or the fabrication process. The approach can be also used to assess the integrity of existing components that have developed cracks by computing the likelihood of crack initiation. The proposed approach can be expanded to other steel grades that are typically used in steel construction. Moreover, in line with Performance-Based Design, the code provisions should incorporate acceptable probabilities of crack initiation to evaluate discontinuities, which are established according to the objective of the building performance instead of a prescriptive fracture toughness value.

References

- [1] Zehnder AT. Fracture mechanics: Lecture notes in applied and computational mechanics: Springer; 2012.
- [2] ANSI/AISC 360-10. AISC 360-10. Specification for structural steel buildings. Chicago, IL, USA.: American Institute of Steel Construction; 2010.
- [3] CAN/CSA-S16-14. Design of steel structures. Mississauga, ON: Canadian Standards Association; 2014.
- [4] AWS D1.1. AWS D1.1 2010. Structural welding code—steel. Miami, FL, USA.: American Welding Society; 2010.
- [5] CAN/CSA-W59. CAN/CSA W59-13 Welded steel construction. Mississauga, Ont.: Canadian Standards Association; 2013.
- [6] Ibrahim OA, Lignos DG, Rogers CA. Proposed modeling approach of welding procedures for heavy steel plates (Submitted). Eng Struct. 2015.
- [7] Suwan S. Analysis of structural plate mechanical properties : statistical variability and implications in structural reliability [M S in Engineering]: University of Texas at Austin; 2002.
- [8] Barsom JM, Rolfe ST. Fracture and fatigue control in structures : applications of fracture mechanics. 2nd ed. Englewood Cliffs, N.J.: Prentice-Hall; 1987.
- [9] ASTM A572 Gr.50. A572/A572M-13a Standard Specification for High-Strength Low-Alloy Columbium-Vanadium Structural Steel. 2013.
- [10] ASTM A913 Gr.65. A913/A913M-14a Standard Specification for High-Strength Low-Alloy Steel Shapes of Structural Quality, Produced by Quenching and Self-Tempering Process. 2014.
- [11] Murakami Y. Stress intensity factors handbook. 1st ed. Oxford Oxfordshire ; New York: Pergamon; 1987.
- [12] Tada H, Paris PC, Irwin GR. The stress analysis of cracks handbook. 3rd ed. New York: ASME Press; 2000.
- [13] Chatterjee S, Hadi AS. Regression analysis by example. 4th ed. Hoboken, N.J.: Wiley-Interscience; 2006.
- [14] Benjamin JR, Cornell CA. Probability, statistics, and decision for civil engineers. New York,: McGraw-Hill; 1970.
- [15] ASTM A588 Gr.B. ASTM A588/A588M-10 Standard Specification for High-Strength Low-Alloy Structural Steel, up to 50 ksi [345 MPa] Minimum Yield Point, with Atmospheric Corrosion Resistance. 2010.
- [16] Nikolaidou V, Rogers CA, Lignos DG. Finite element modeling of welding procedures in high strength W-Shapes. Canadian Society of Civil Engineering, 3rd Specialty Conference on Material Engineering and Applied Mechanics. Montreal, Quebec2013.
- [17] ASTM A370. A370-14 Standard Test Methods and Definitions for Mechanical Testing of Steel Products. 2014.
- [18] Phillips DT. Applied goodness of fit testing: American Institute of Industrial Engineers; 1972.
- [19] Montgomery DC, Runger GC. Applied Statistics and Probability for Engineers 6th Edition: John Wiley and sons Inc.; 2014.
- [20] Crow EL, Davis FA, Maxfield MW. Statistics manual : with examples taken from ordnance development. New York: Dover; 1960.

- [21] Bannister AC, Steel B. Structural Integrity Assessment Procedures for European Industry: SINTAP : Sub-task 3.3 Report : Final Issue Determination of Fracture Toughness from Charpy Impact Energy: Procedure and Validation: British Steel plc; 1998.
- [22] BS 7910:2005. Guide to methods for assessing the acceptability of flaws in metallic structures'. BSI; 2005.
- [23] Mathworks. Matlab R2012b. version 8.0 ed: The MathWorks Inc.; 2012.
- [24] Jefferson TB, Woods G. Metals and how to weld them. 2d ed. Cleveland,: James F. Lincoln Arc Welding Foundation; 1962.

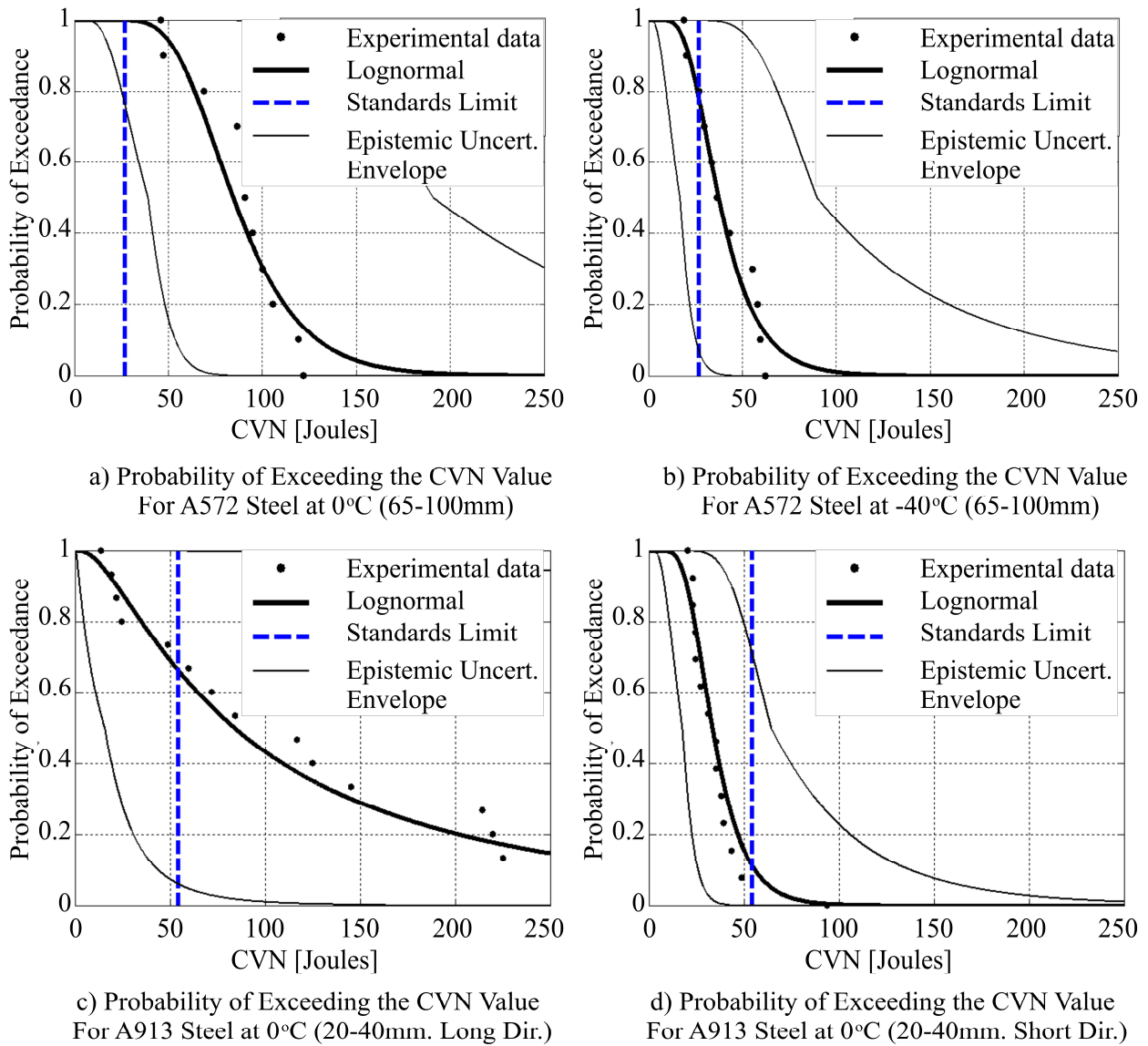
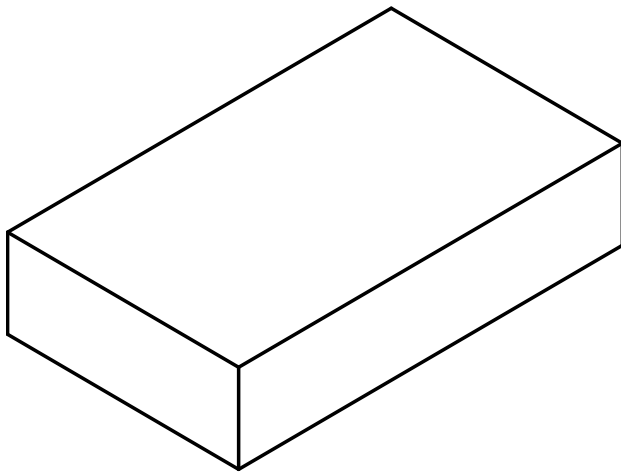
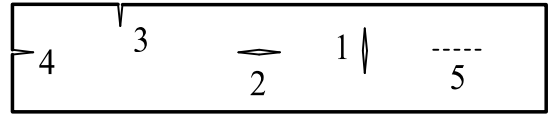


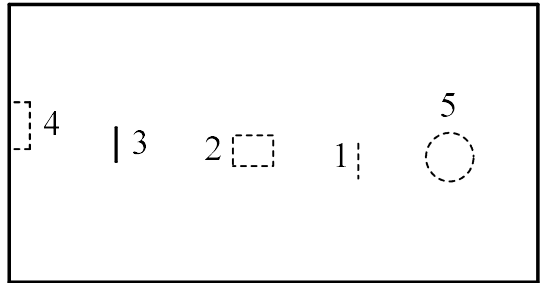
Figure 1: Epistemic uncertainty of CVN Data with 5% and 95% confidence interval (data from [6, 7, 16]).



a) 3D View of Plate

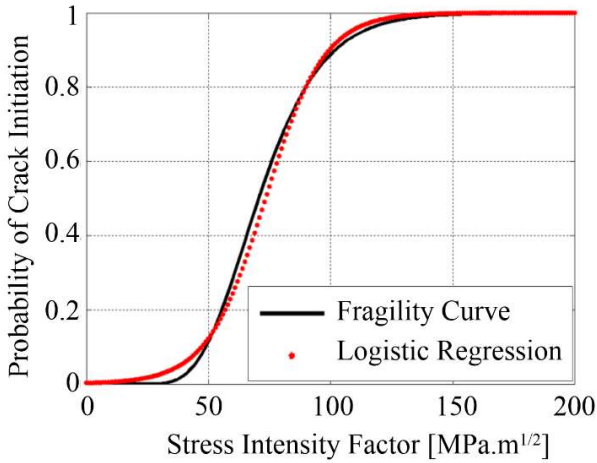


b) Elevation View of Plate

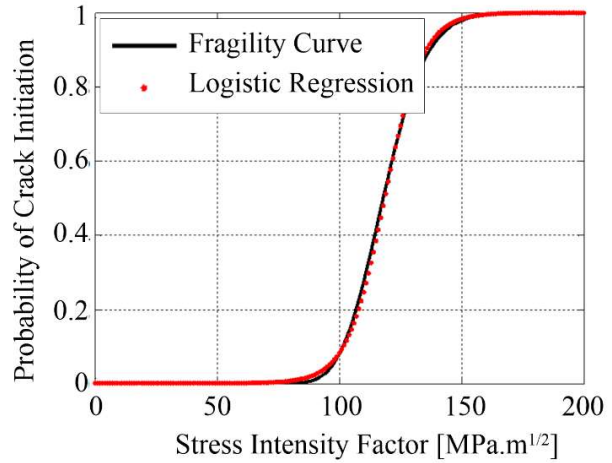


c) Plan View of Plate

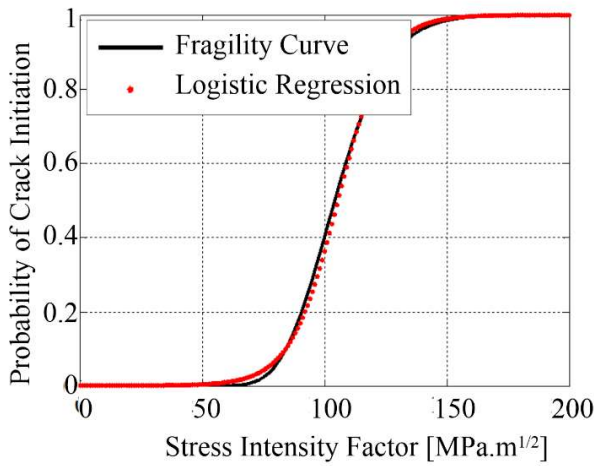
Figure 2: Illustration of considered crack types.



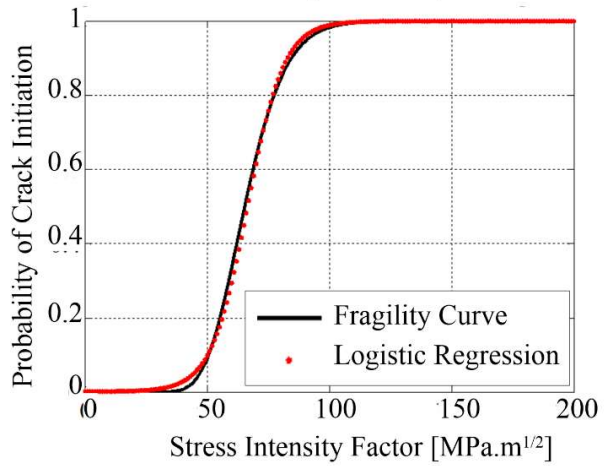
a) Comparison Between the Logistic Reg. Formula and the Crack Fragility Curve For A572 Steel at 21/-40°C (65-100mm)



b) Comparison Between the Logistic Reg. Formula and the Crack Fragility Curve For A588 Steel at 21/-40°C (65-100mm)



c) Comparison Between the Logistic Reg. Formula and the Crack Fragility Curve For A572 Steel at 0/-60°C (2013)



d) Comparison Between the Logistic Reg. Formula and the Crack Fragility Curve For A913 Steel at 0/-48°C (2013)

Figure 3: A comparison between the crack initiation fragility curves and the logistic regression formula.

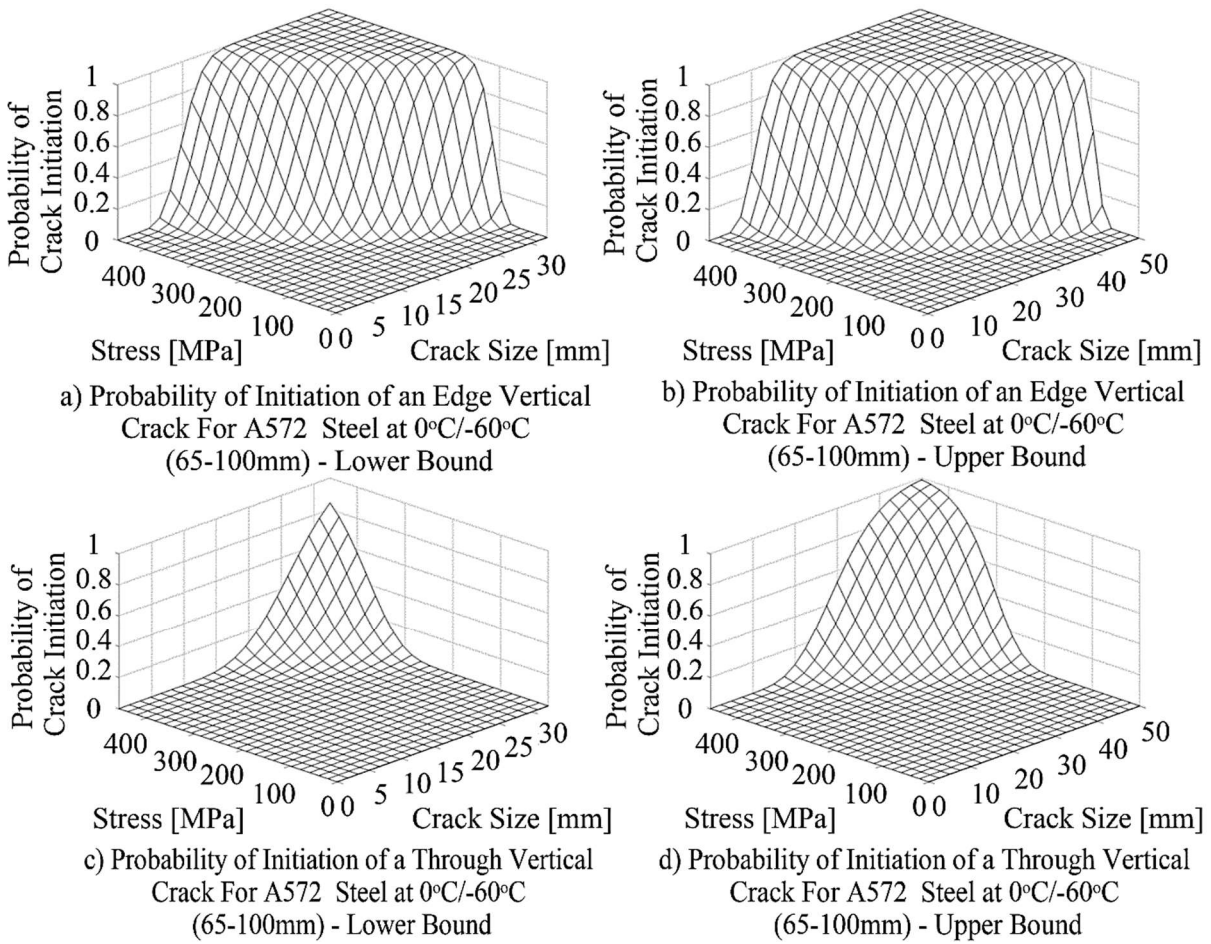


Figure 4: Impact of the crack type on the probability of crack initiation showing the upper and lower bound probabilities of crack types 1 and 3 for the ASTM A572 Gr. 50 steel ($f_y=345$ MPa) (dynamic/static temperatures) based on tests conducted at McGill University [6, 16].

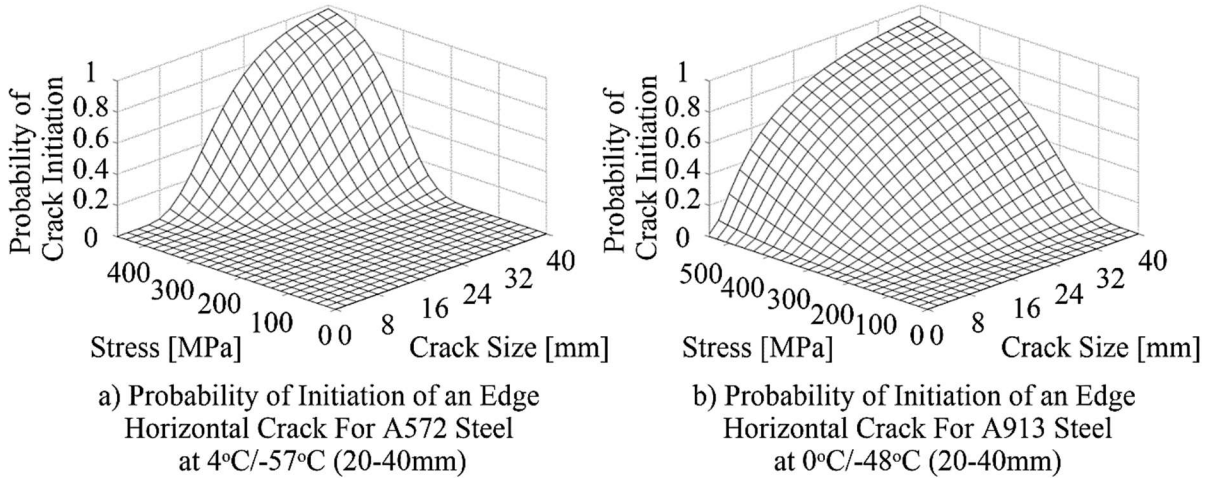


Figure 5: Impact of material type on the probability of crack type 4 initiation for the ASTM A572 Gr. 50 steel ($f_y= 345$ MPa) and ASTM A913 Gr. 65 steel ($f_y= 450$ MPa) (dynamic/static temperatures).

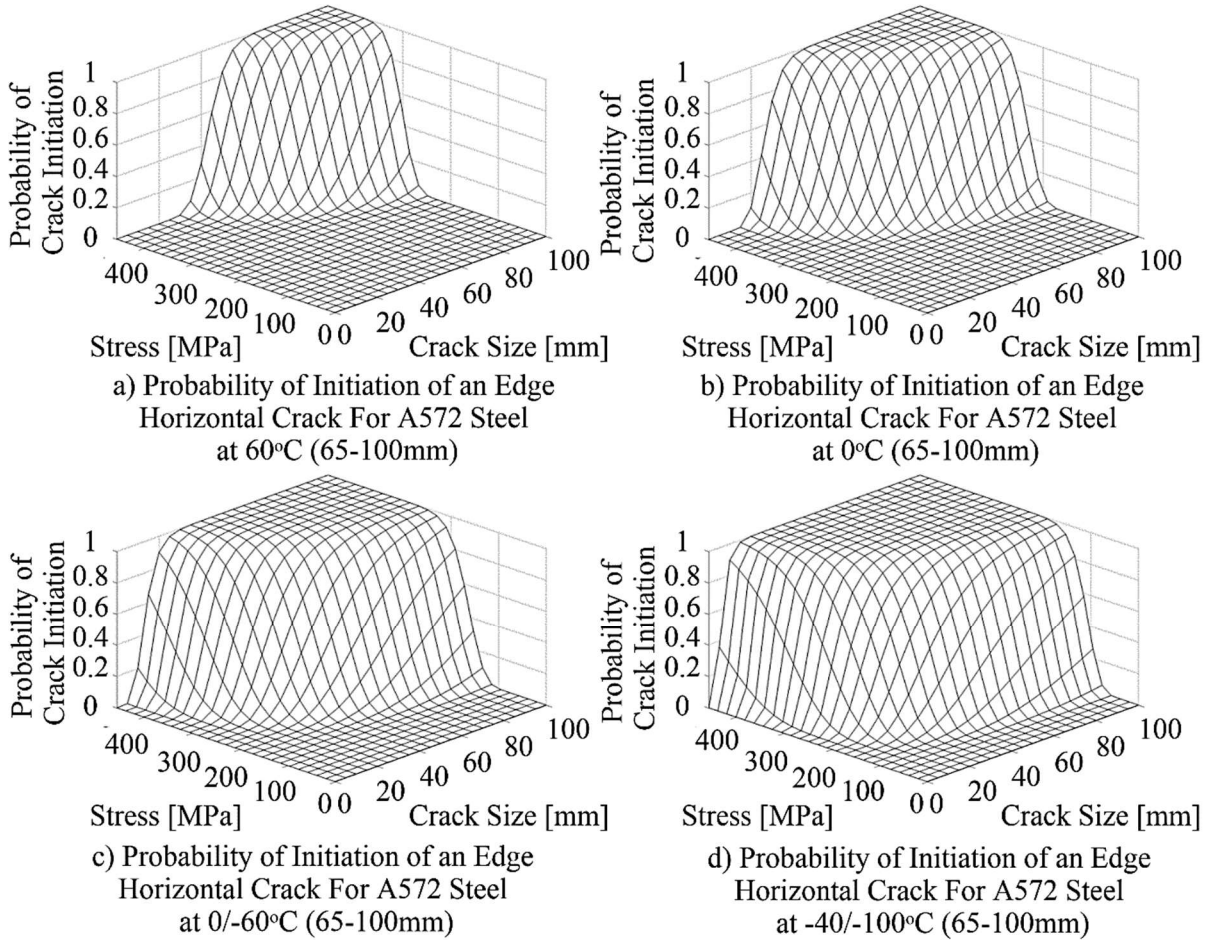


Figure 6: Impact of temperature on the probability of crack type 4 initiation for the ASTM A572

Gr. 50 steel ($f_y = 345$ MPa) (dynamic/static temperatures) based on tests conducted at McGill

University [6, 16].

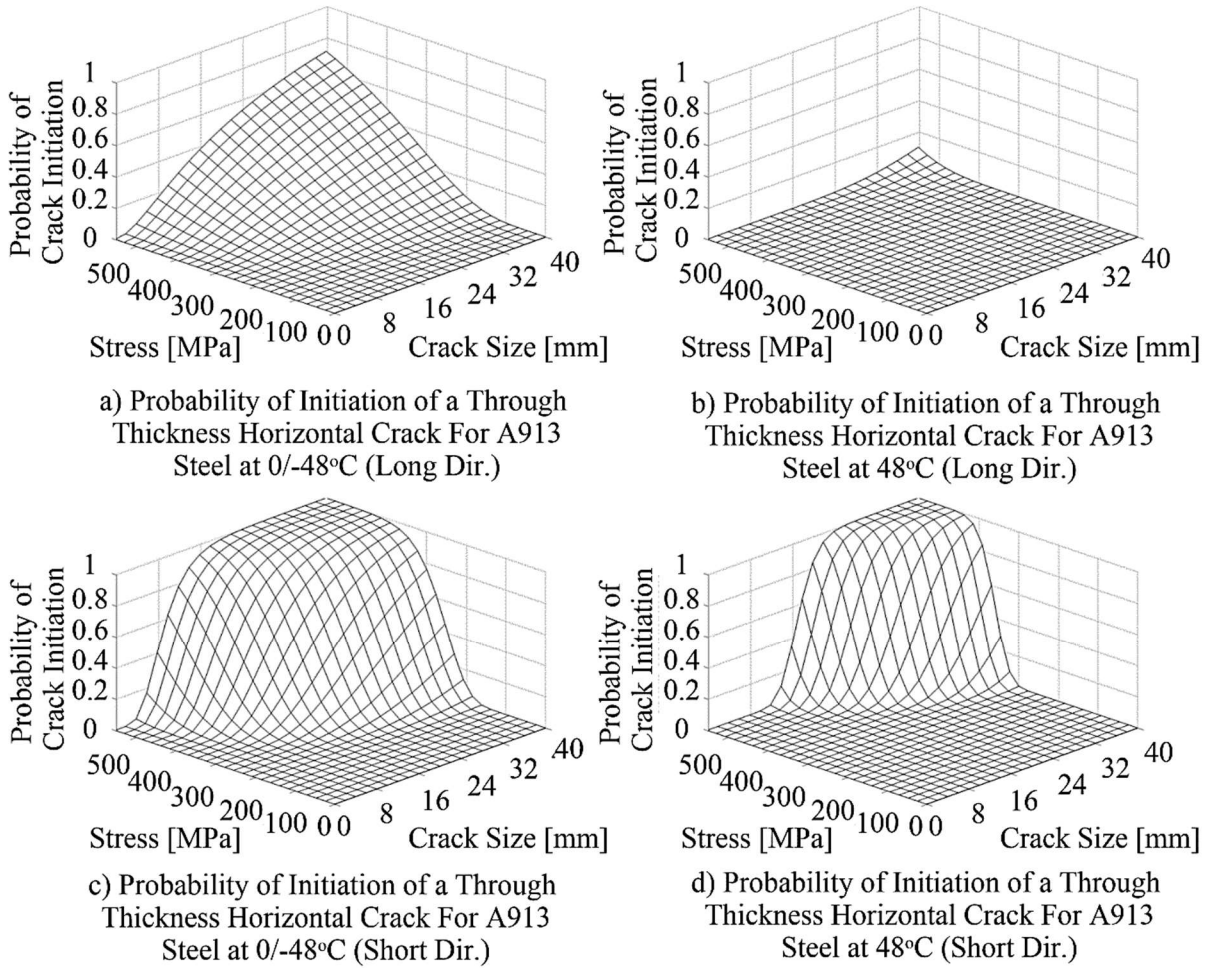


Figure 7: Impact of grain direction on the upper and lower shelf probabilities of initiation of crack type 2 for the ASTM A913 Gr. 65 steel ($f_y= 450$ MPa) in long and short grain directions (dynamic/static temperatures) according to tests conducted at McGill University [6, 16].

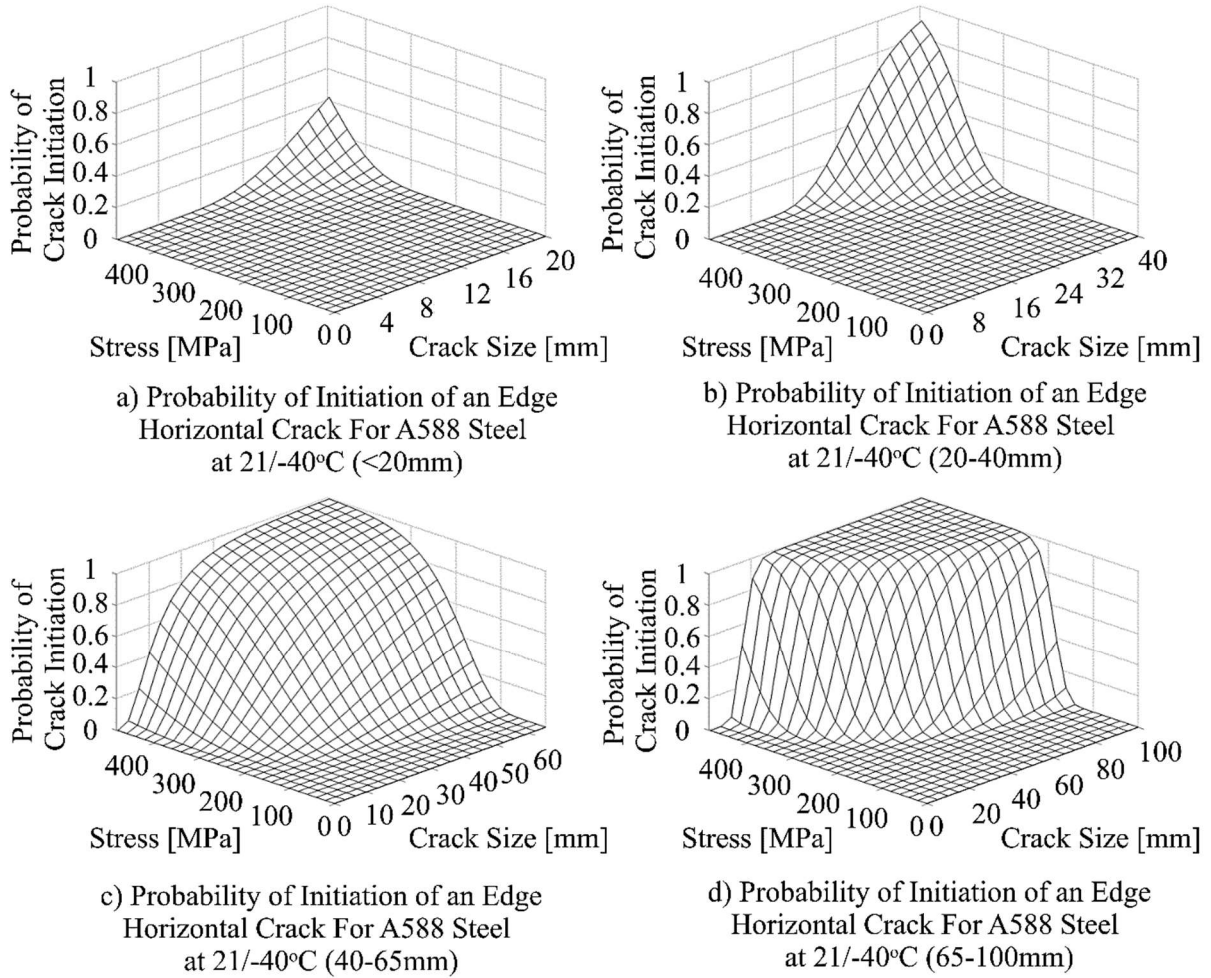


Figure 8: Impact of plate thickness on the probability of initiation of crack type 4 for ASTM A588 Gr. B steel ($f_y = 345$ MPa) (dynamic/static temperatures) according to tests conducted by Suwan [7].

Table 1: Summary of the results of the lognormal distribution of energy for ASTM A572 Gr. 50 steel and ASTM A588 Gr. B steel for CVN tests conducted by Suwan [7]

	Mean ($\mu_{5\%} - \mu - \mu_{95\%}$)	St. Dev. ($\beta_{5\%} - \beta - \beta_{95\%}$)	No. Specimens
A572 Gr. 50 ($f_y=345$ MPa) Thickness Group: < 20mm			
-18°C	138 – 67 – 35 J	0.83 – 0.94 – 1.07	91
4°C	174 – 99 – 59 J	0.60 – 0.68 – 0.78	91
21°C	199 – 130 – 86 J	0.44 – 0.49 – 0.56	91
A572 Gr. 50 ($f_y=345$ MPa) Thickness Group: 20-40mm			
-18°C	126 – 71 – 41 J	0.58 – 0.66 – 0.77	70
4°C	172 – 119 – 83 J	0.34 – 0.39 – 0.45	70
21°C	204 – 149 – 108 J	0.28 – 0.32 – 0.37	70
A572 Gr. 50 ($f_y=345$ MPa) Thickness Group: 40-65mm			
-18°C	109 – 3.81 – 21 J	0.90 – 1.03 – 1.21	63
4°C	196 – 66 – 26 J	0.85 – 1.00 – 1.20	49
21°C	383 – 126 – 48 J	0.63 – 0.75 – 0.94	35
A572 Gr. 50 ($f_y=345$ MPa) Thickness Group: 65-100mm			
-18°C	29 – 17 – 10 J	0.30 – 0.40 – 0.59	14
4°C	63 – 29 – 14 J	0.37 – 0.48 – 0.71	14
21°C	111 – 39 – 16 J	0.44 – 0.57 – 0.85	14
A588 Gr. B ($f_y=345$ MPa) Thickness Group: < 20mm			
-18°C	148 – 86 – 52 J	0.65 – 0.72 – 0.82	105
4°C	193 – 127 – 85 J	0.47 – 0.52 – 0.59	105
21°C	209 – 153 – 113 J	0.34 – 0.38 – 0.43	105
A588 Gr. B ($f_y=345$ MPa) Thickness Group: 20-40mm			
-18°C	217 – 125 – 74 J	0.58 – 0.65 – 0.74	91
4°C	256 – 179 – 126 J	0.35 – 0.39 – 0.45	91
21°C	254 – 197 – 152 J	0.25 – 0.28 – 0.32	91
A588Gr. B ($f_y=345$ MPa) Thickness Group: 40-65mm			
-18°C	98 – 41 – 19 J	0.80 – 0.93 – 1.12	49
4°C	135 – 58 – 28 J	0.69 – 0.81 – 0.97	49
21°C	169 – 79 – 40 J	0.59 – 0.69 – 0.83	49
A588 Gr. B ($f_y=345$ MPa) Thickness Group: 65-100mm			
-18°C	100 – 37 – 15 J	0.42 – 0.55 – 0.82	14
4°C	151 – 65 – 29 J	0.32 – 0.42 – 0.62	14
21°C	181 – 108 – 65 J	0.18 – 0.23 – 0.35	14

Table 2: Summary of the results of the lognormal distribution of energy for ASTM A572 steel Gr. 50 and ASTM A913 Gr. 65 steel for CVN tests conducted at McGill University [6, 16]

	Mean ($\mu_{5\%} - \mu - \mu_{95\%}$)	St. Dev. ($\beta_{5\%} - \beta - \beta_{95\%}$)	No. Specimens
A572 Gr. 50 ($f_y=345$ MPa)			
-60°C	28 – 11 – 5 J	0.43 – 0.60 – 1.02	9
-40°C	90 – 37 – 17 J	0.32 – 0.43 – 0.69	11
0°C	191 – 85 – 39 J	0.25 – 0.33 – 0.53	11
60°C	208 – 164 – 128 J	0.12 – 0.15 – 0.19	28
81°C	191 – 156 – 126 J	0.11 – 0.13 – 0.17	29
A913 Gr. 65 ($f_y=450$ MPa) Long direction			
0°C	914 – 84 – 15 J	0.81 – 1.05 – 1.50	16
21°C	399 – 121 – 42 J	0.43 – 0.56 – 0.79	17
48°C	420 – 150 – 58 J	0.31 – 0.40 – 0.61	13
69°C	479 – 162 – 60 J	0.26 – 0.36 – 0.59	10
A913 Gr. 65 ($f_y=450$ MPa) Short direction			
0°C	64 – 33 – 17 J	0.31 – 0.40 – 0.60	14
21°C	83 – 43 – 22 J	0.30 – 0.39 – 0.57	15
48°C	52 – 40 – 31 J	0.11 – 0.15 – 0.22	14
69°C	48 – 39 – 31 J	0.10 – 0.13 – 0.19	15

Table 3: Maximum difference in probability between empirical results and the distribution compared to the KS-test limit with 5% significance for ASTM A572 Gr. 50 steel tests by Suwan [7]

Thickness Group: < 20mm				
Distribution	Lognormal	Weibull	Exponential	Limit (5%)
-18°C	0.099	0.110	0.088	0.128
4°C	0.132	0.099	0.209	0.128
21°C	0.121	0.066	0.286	0.128
Thickness Group: 20-40mm				
Distribution	Lognormal	Weibull	Exponential	Limit (5%)
-18°C	0.086	0.071	0.243	0.146
4°C	0.114	0.071	0.343	0.146
21°C	0.129	0.143	0.400	0.146

Table 4: Values of B_0 and B_1 and the deviance of the logistic regression for ASTM A572 Gr. 50 and ASTM A588 Gr. B steel according to tests conducted by Suwan [7]

Thickness	Temperature	B_0	B_1	Deviance	Max. Residual
A572 Gr. 50 ($f_y=345$ MPa)					
t<20mm	-18°C (-79°C)*	-3.59	0.035	6.74	0.085
	4°C (-57°C)*	-5.16	0.043	3.92	0.070
	21°C (-40°C)*	-7.22	0.054	2.03	0.056
t=20-40mm	-18°C (-79°C)*	-5.31	0.053	3.15	0.069
	4°C (-57°C)*	-9.29	0.074	1.07	0.047
	21°C (-40°C)*	-11.35	0.081	0.76	0.042
t=40-65mm	-18°C (-79°C)*	-3.16	0.037	7.19	0.090
	4°C (-57°C)*	-3.35	0.033	7.47	0.088
	21°C (-40°C)*	-4.69	0.035	5.19	0.075
t=65-100mm	-18°C (-79°C)*	-9.06	0.189	0.43	0.048
	4°C (-57°C)*	-7.42	0.119	0.89	0.055
	21°C (-40°C)*	-6.18	0.084	1.62	0.062
A588 Gr. B ($f_y=345$ MPa)					
t<20mm	-18°C (-79°C)*	-4.8	0.043	4.31	0.073
	4°C (-57°C)*	-6.79	0.051	2.32	0.058
	21°C (-40°C)*	-9.52	0.066	1.15	0.047
t=20-40mm	-18°C (-79°C)*	-5.48	0.041	3.79	0.068
	4°C (-57°C)*	-9.14	0.059	1.36	0.048
	21°C (-40°C)*	-12.95	0.081	0.67	0.039
t=40-65mm	-18°C (-79°C)*	-3.54	0.044	5.69	0.086
	4°C (-57°C)*	-4.21	0.045	4.77	0.079
	21°C (-40°C)*	-5.054	0.047	3.70	0.071
t=65-100mm	-18°C (-79°C)*	-6.39	0.089	1.46	0.060
	4°C (-57°C)*	-8.57	0.092	0.95	0.050
	21°C (-40°C)*	-15.39	0.129	0.36	0.036

* The temperature between brackets is the shifted temperature for static loading

Table 5: Values of B_0 and B_1 and the deviance of the logistic regression for A572 Gr. 50 steel according to tests conducted at McGill University [6]

Temperature	B_0	B_1	Deviance	Max. Residual
-60°C (-120°C)*	-5.90	0.148	0.98	0.051
-40°C (-100°C)*	-8.33	0.118	0.77	0.064
0°C (-60°C)*	-10.87	0.103	0.63	0.043
0°C (interpolated)	-15.84	0.108	2.75	0.023
21° C (interpolated)	-18.06	0.111	2.34	0.021
60°C	-24.14	0.127	0.27	0.030
81°C	-27.01	0.146	0.23	0.030

* The temperature between brackets is the shifted temperature for static loading

Table 6: Values of B_0 and B_1 and the deviance of the logistic regression for ASTM A913 Gr. 65 steel according to tests conducted at McGill University [16]

Position	Temperature	B_0	B_1	Deviance	Max. Residual
Parallel to rolling direction	0°C (-48°C)*	-3.26	0.028	8.21	0.089
	21°C (-27°C)*	-6.38	0.049	2.64	0.061
	48°C	-8.82	0.042	1.92	0.049
	69°C	-9.97	0.046	1.53	0.046
Perpendicular to rolling direction	0°C (-48°C)*	-8.96	0.134	0.61	0.049
	21°C (-27°C)*	-9.21	0.121	0.65	0.048
	48°C	-21.56	0.211	0.17	0.032
	69°C	-25.32	0.251	0.14	0.030

* The temperature between brackets is the shifted temperature for static loading